

RESILIENCY EVALUATION OF REINFORCED CONCRETE BUILDINGS

Susumu Kono¹, Ryo Kuwabara¹, Fuhito Kitamura¹, Eko Yuniarisyah¹,
Hidekazu Watanabe², Tomohisa Mukai², David Mukai³
Tokyo Institute of Technology¹, Building Research Institute²,
Univ. of Wyoming (Visiting professor at Tokyo Institute of Technology)³
Yokohama, Japan¹; Tsukuba, Japan²; Laramie, USA³

Abstract

A numerical procedure employed FEM analysis results on a real scale five-story reinforced concrete frame building in order to simulate complete residual flexural crack profile simulation (crack spacing, width, and length). The computed crack profile is compared to the experimental results through crack area damage ratio, which is a proposed damage index. Although number of cracks and their width were well simulated for different levels of loading stages, the crack area damage was hard to simulate at this moment. Nevertheless, the discussion will be helpful to evaluate cost of repair after earthquake damage. The paper describes a part of current research efforts on resilient reinforced concrete structures in Japan by simulating damage of reinforced concrete members such as cracks and spalling of concrete, or yielding and buckling of reinforcement for different limit states. It is interesting to see how to utilize secondary RC walls to improve seismic performance for damage reduction by changing their configuration and rebar arrangement. It can be seen that strength enhancement with ductile detailing is one of the easiest and economical solutions to reduce seismic damage for ordinary reinforced concrete buildings.

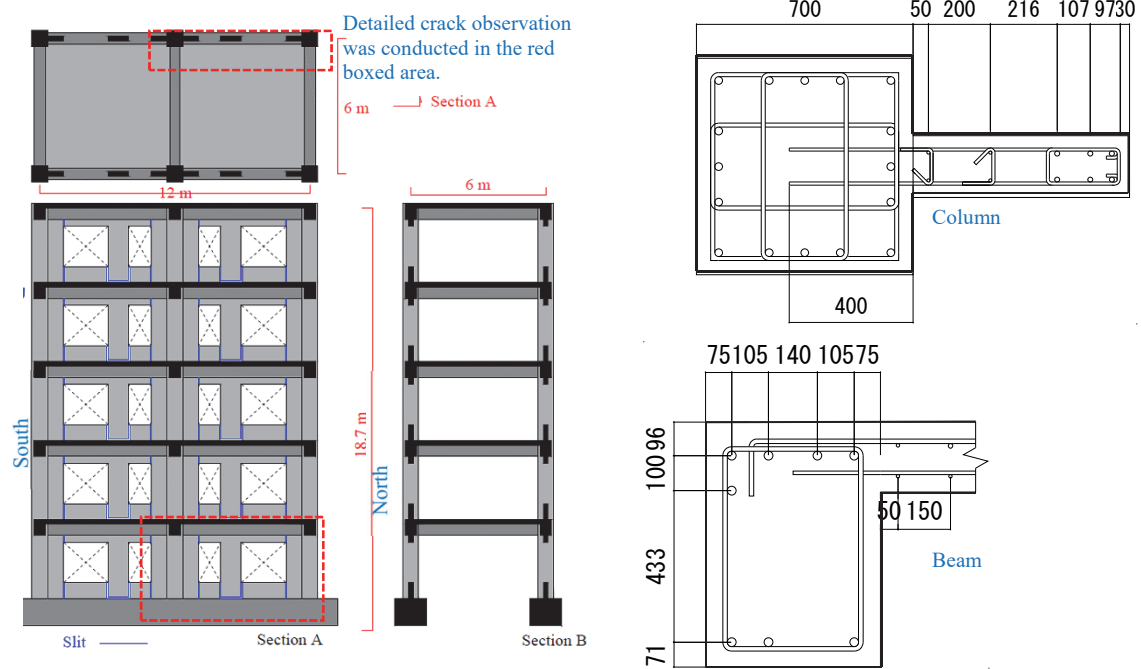
Introduction

Damage to non-structural (or secondary) members are as important as that to structural members from the view point of continuous post-earthquake functionality of buildings. Resilience of building structures specifically means low or no damage of structural and non-structural (or secondary) members and quick recovery of functions of buildings. In order to achieve resilient building structures, it is important to develop low damage structural systems in a broader sense and propose design procedures to advance the idea.

Engineers in National Institute for Land and Infrastructure Management (NILIM) and Building Research Institute (BRI) designed and tested real scale five story reinforced concrete buildings to study seismic performance of strength-based building system. Three universities and seven companies joined the experimental works at BRI to closely observe damage at different loading stages. The building introduced in this paper was tested in 2014 (Kabayasawa et al. 2016 and 2017). The designed concrete frame building had higher load carrying capacity by adding wing walls to columns, or standing or/and hanging walls to beams. It was supposed to possess load carrying capacity equivalent to $C_0=0.45 - 0.55$ (C_0 : base shear coefficient) at mechanism formation with maximum interstory drift as small as 0.4% - 0.8%. This implies that the building would have an elastic or nearly elastic response even under large scale earthquakes. Limited deformation would result in dramatic damage reduction in columns, beams, and beam-column connections. This paper discusses features of cracks from a numerical view point. A crack simulation procedure is introduced by revising the former strain based concept (Kono et al. 2017). The main content of this paper was published in the paper (Kono et al. 2018) but some revisions were made.

Experimental work

Figure 1 shows configuration of a five-story RC specimen and typical section size with reinforcement arrangement. It is noted that the building had structural slits (or gaps) between secondary walls as shown by thick blue lines in Figure 1(a). Cracks were traced and copied to transparencies and the maximum width for each crack was recorded (Figure 2).

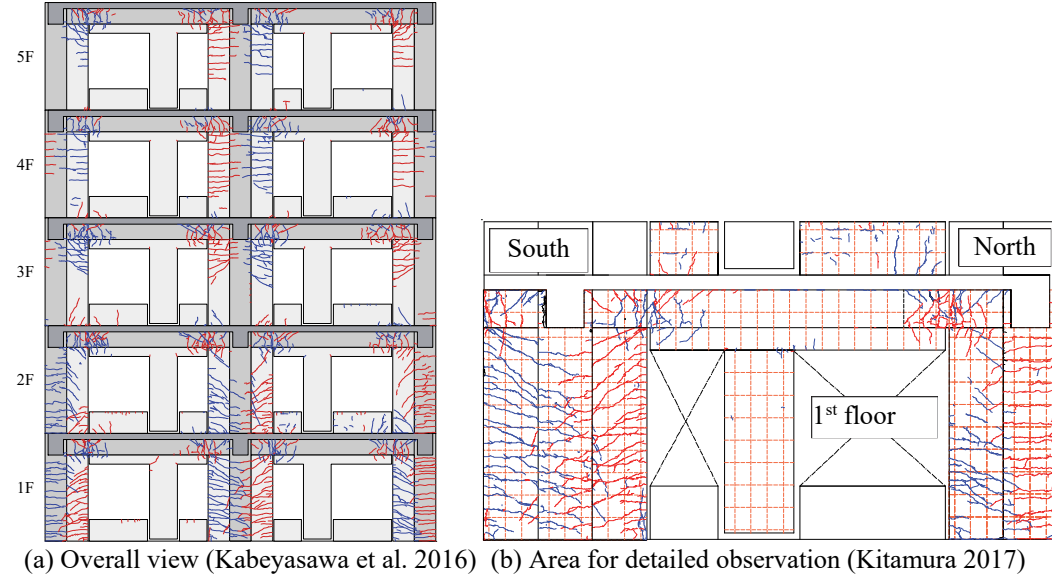


(a) Specimen configuration

b) Column with a wing wall and beam with one side slab

Figure 1. Configuration of the 2014 five story specimen and typical section size (Fukuyama et al. 2015).

1/100



(a) Overall view (Kabeyasawa et al. 2016) (b) Area for detailed observation (Kitamura 2017)

Figure 2. Recorded cracks and spalling at R=1%.

Simulation of flexural cracks

The paper aims to obtain complete residual flexural and shear crack profiles (crack spacing, width, and length) using FEM analysis results. A procedure to evaluate residual cracks is introduced in Figure 3.

The flow has two branches; branch for residual flexural crack profiles and branch for residual shear crack profiles. Yellow boxes (#3, 5, and 10) are predetermined values and a red box (#6) is obtained from a regression analysis. Crack spacing (#3) is determined based on CEB-FIP Model Code equation (1978) although the crack spacing in this code is not necessarily for seismic purposes. Horizontal crack length, $L_{h(i)}$, is taken into consideration (#7-1) when crack width is larger than visible flexural crack width $W_{limit} = 0.01\text{mm}$ (#5). Then actual diagonal and meandering crack length, $L_{f(i)}$, is obtained (#7-2) by multiplying correction factor, α , which is obtained from a regression analysis (#6). From #3, #4, and #7-2, complete residual flexural crack profiles (spacing, width, and length) are obtained. Similar procedure may be taken for shear cracks although it is not explained in detail in this paper.

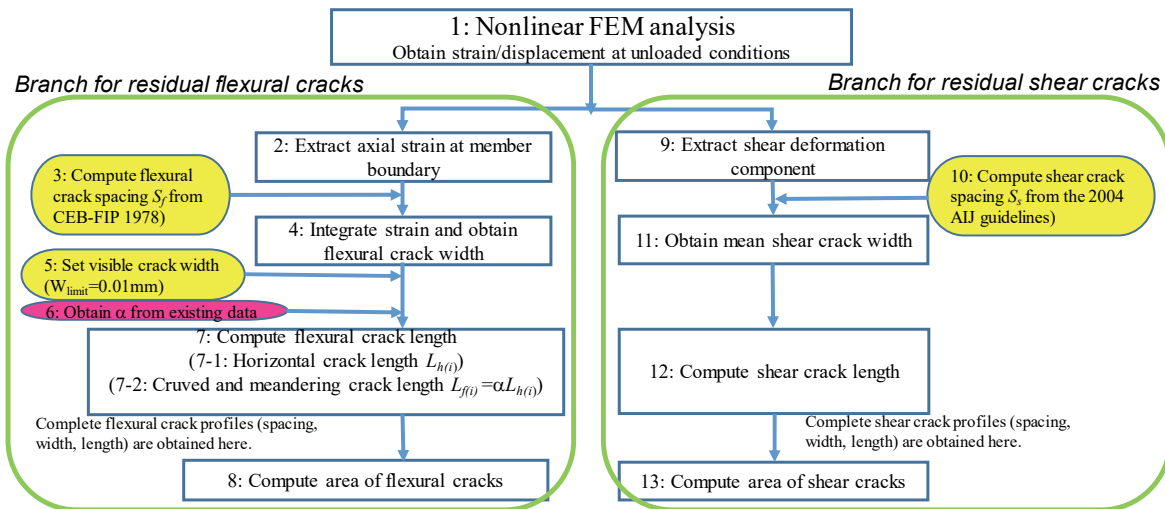


Figure 3. Flow chart how to obtain complete residual flexural crack profiles.

Numerical analysis with an FEM program. (#1 in Figure 3)

Figure 4 shows a 2D finite element mesh used in a commercial FEM program “FINAL” (ITOCHU 2016). Concrete was modeled as isoparametric quadrilateral elements with smeared reinforcement, and longitudinal reinforcement was modeled as beam-column elements. Perfect bond characteristics were assumed for all reinforcement. All degrees of freedom were fixed at nodes on the bottom face of the foundation beams. Self-weight was applied as concentrated load at beam-column connections based on a tributary area. Lateral load was applied at the central beam-column connections of roof and fourth floor by 1:2 ratio to simulate the load conditions in experiment. Load was controlled by the lateral displacement of the roof level and loading protocol followed the measured displacement although the second cycle, which the experimental loading protocol had, was skipped to save computational time. The numerical simulation was carried out up to R=1% since the resisting mechanism of building changed when structural slits (or gaps) closed at R=+1.3% in experiment. The elements employed default material models; modified Ahmad model (Naganuma 1995) and Izumo model (Izumo et al. 1987) were used for concrete and modified Menegotto-Pinto model (Ciampi et al. 1982) was used for reinforcement.

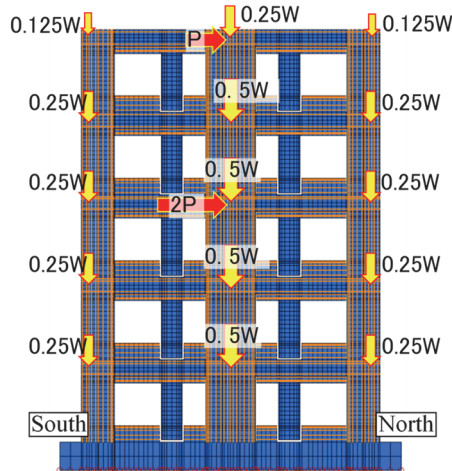


Figure 4. Finite element mesh and loading condition in 2D finite element analysis (Kitamura 2017).

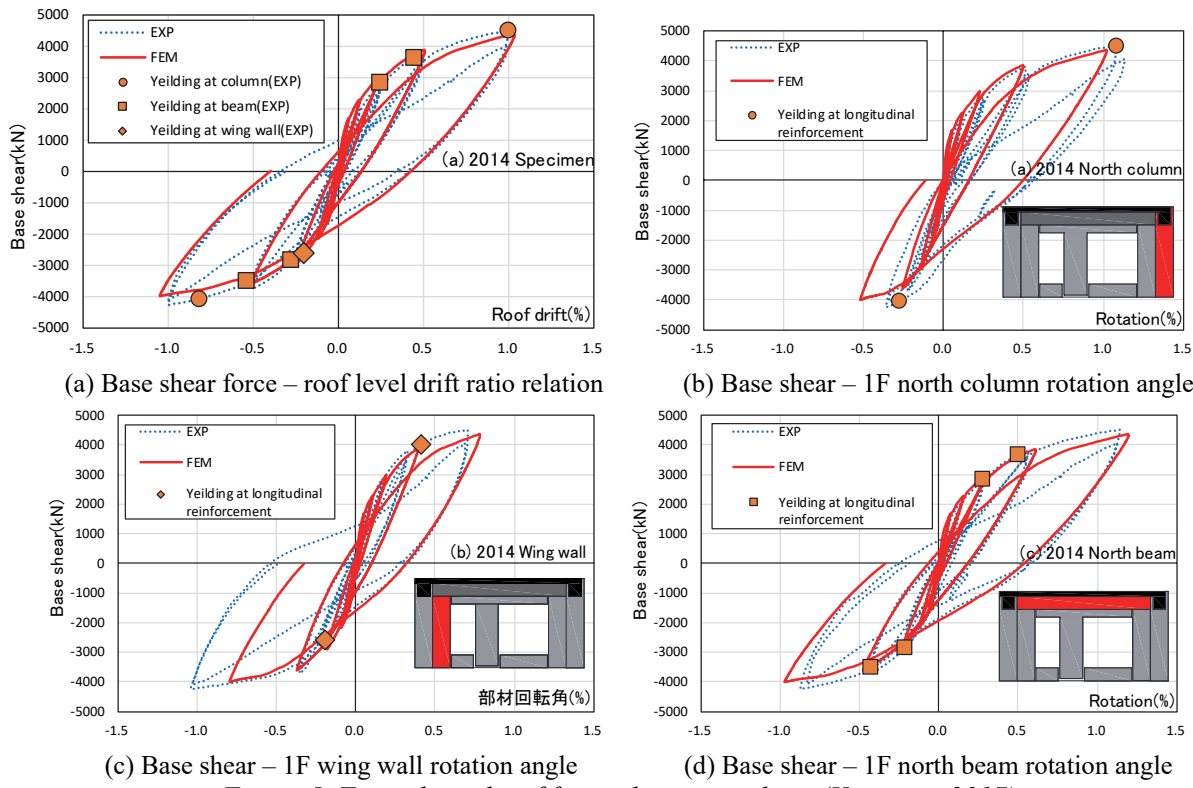


Figure 5. Typical results of finite element analysis (Kitamura 2017).

Figure 5(a) shows base shear force – roof level drift relation up to 1% drift. The numerical simulation agrees well with the experimental results. Figure 5(b)(c)(d) show the base shear force – member rotation of the north column (1F), wing wall (1F), and north beam(2F). The deformation of each member directly influences the simulation of crack performance. The simulated curves agrees relatively well with the experimental results in the positive side but did not agree very well in the negative side.

Numerical simulation of flexural cracks. (#2 ~7 in Figure 3)

Most cracks were governed by flexure as can be seen in Figure 2 and crack simulation in this paper treated only flexural cracks. An effect of some flexural-shear cracks was considered with conversion

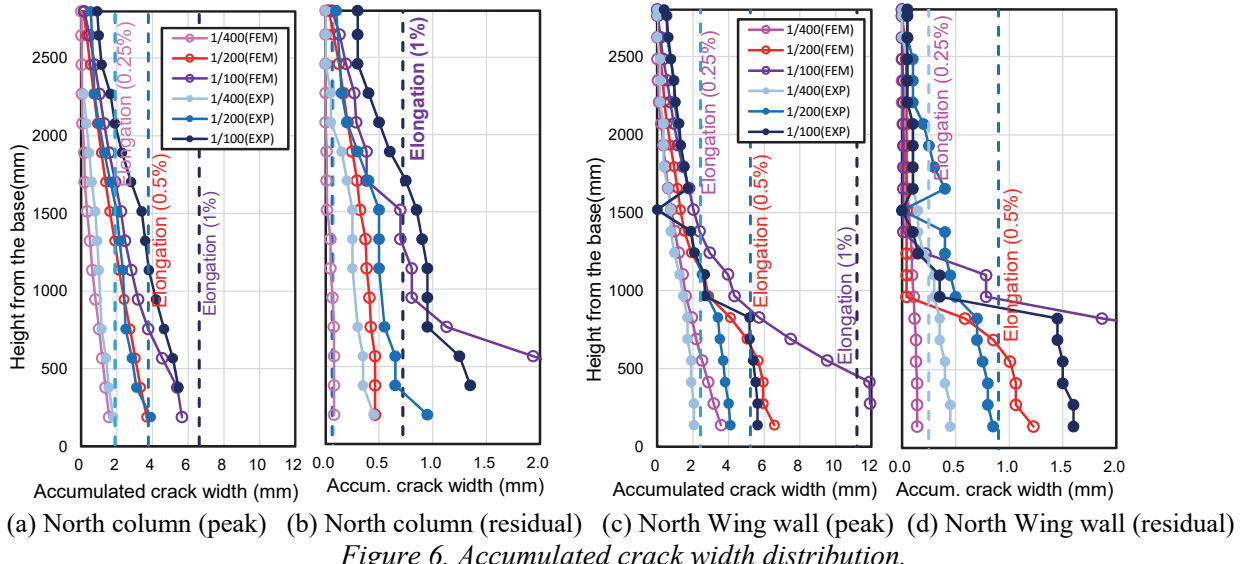
index, α , which is explained later. The first floor column is used as an example to explain how to obtain spacing, width, and length of flexural cracks.

First, crack spacing and width (#2, 3, and 4 in Figure 3) is explained step by step. Width of the i -th crack, W_i , was computed based on Eq. (1). It was assumed that concrete does not deform and elongation of a member comes from crack openings. Hence, strain obtained from the finite element analysis represents effects of smeared cracks. Based on this assumption, the flexural crack width of a member can be obtained by integrating longitudinal tensile strain (ε_{zz}) over crack spacing (S_{rm}). The crack spacing is based on Eq. (2) proposed in CEB-FIP Model Code (CEB-FIP 1978). Equation (2) is based on the condition that the number of cracks reached saturated condition. The error of Eq. (2) was studied beforehand and turned out to be reasonably small after $R=0.25\%$.

$$W_i = \int_{h_i-S_f/2}^{h_i+S_f/2} \varepsilon_{zz} dz \quad (1)$$

$$S_f = 2 \left(c_s + \frac{s_y}{10} \right) + k_1 k_2 \frac{d_{by}}{p_y} \quad (2)$$

where W_i and h_i are width and height of the i -th crack, ε_{zz} is tensile strain in vertical (z) direction, S_f is crack spacing. Other notations in Eq. (2) should be referred to the original document. Figure 6 shows accumulated crack width for the north column (1F) and the wing wall (1F). Crack width was accumulated from the top to bottom in the figure. The accumulated crack width at the bottom is close to the elongation measured by displacement gages, and measured elongation of member is expressed by the vertical break lines in the figure. Figure 6(a) and (c) show variations at the peaks and Figure 6(b) and (d) show those at the unloaded conditions. Each figure has comparisons between experimental and analytical results for three drift levels at $R=0.25\%$, 0.5% and 1% . Solid circles on the experimental curves show the location of actual cracks and those for analysis show simulated points with spacing, S_f . Simulated variations for peak load agreed relatively well with experimental results for the column and wing wall. However, the agreement is not very good for residual crack width. If the total elongation of the tension fiber in analysis does not agree with experimental results, the simulation does not agree with the experimental results.



Secondly, crack length simulation (#5, 6, and 7 in Figure 3) is explained. Crack length was computed using FEM analysis results. The crack is assumed visible when crack width of the i -th crack exceeds the limit crack width, W_{limit} , which is a constant value and defined in Eq. (3). The projected crack length, $L_{h(i)}$, was computed based on the neutral axis depth, $x_{n(i)}$, and invisible crack length, $x_{limit(i)}$, as shown in Eq. (4) and Figure 7. In this paper, the crack opening profile is assumed triangular as shown in Figure 7(d) and the computing process is based on the edge opening, W_i .

$$W_{limit} = 0.01\text{mm} \text{ in this study} \quad (3)$$

$$L_{h(i)} = D - x_{n(i)} - x_{limit(i)} \quad (4)$$

$$L_{f(i)} = \alpha L_{h(i)} \quad (5)$$

$$\alpha = \alpha_1 \cdot \alpha_2 \quad (6)$$

$$\alpha_1 = average \left(\frac{L_{f(exp)}}{L_{d(exp)}} \right) \text{ (from straight length to meandering length)} \quad (7)$$

$$\alpha_2 = average \left(\frac{L_{d(exp)}}{L_{h(exp)}} \right) \text{ (from horizontal projection to diagonal length)} \quad (8)$$

Conversion index, α , was multiplied to obtain actual diagonal and meandering crack length, $L_{f(i)}$, to take into account the fact that cracks are not smooth nor horizontal. Index, α , was determined from the experimental results and the values were 1.15, 1.28, and 1.51 for the column, wing wall, and beam. Index α_1 and α_2 were computed using regression analysis of experimental data using Eqs. (7) and (8).

Since complete profiles of residual flexural crack profiles are obtained (Crack spacing in #3, residual crack width in #4, and crack length in #7-2 in Figure 3), they are validated with experimental data. Figure 8 shows crack area damage ratio, β_A , which is the ratio of all visible crack area summation, $\sum A_{crack(i)}$, to the concrete surface area, $A_{surface}$. It is a no-dimensional quantity as expressed by Eq. (9). Crack area is defined in Figure 7(d) as a blue trapezoid shape.

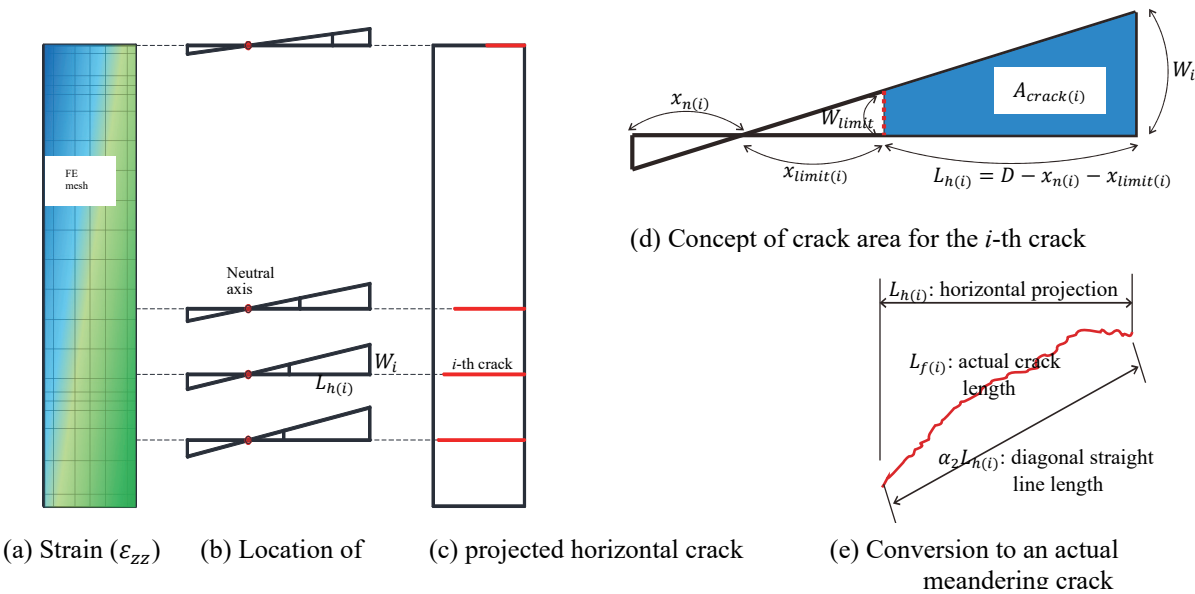


Figure 7. Calculation of crack length.

$$\beta_A = \frac{\sum A_{crack(i)}}{A_{surface}} = \frac{\sum \{0.5 \cdot W_i \cdot (D - x_{n(i)}) - 0.5 \cdot W_{limit} \cdot x_{limit(i)}\}}{A_{surface}} \quad (9)$$

where D is the total depth of a member. Based on the reference (JBDPA 2015), crack width is categorized into four classes of crack width ($0 \leq w_{cr} \leq 0.2mm$, $0.2mm \leq w_{cr} \leq 1mm$, $1mm \leq w_{cr} \leq 2mm$!).

$w_{cr} \geq 2mm^*$ and β_A for each category is expressed as a stack graph in Figure 8. Agreement is not very good but tolerable up to 0.5% drift and is not good at all at 1% drift. It can be seen that the complete crack profiles such as crack damage area ratio is hard to predict even if simulated crack width profiles in Figure 6 are not very bad.

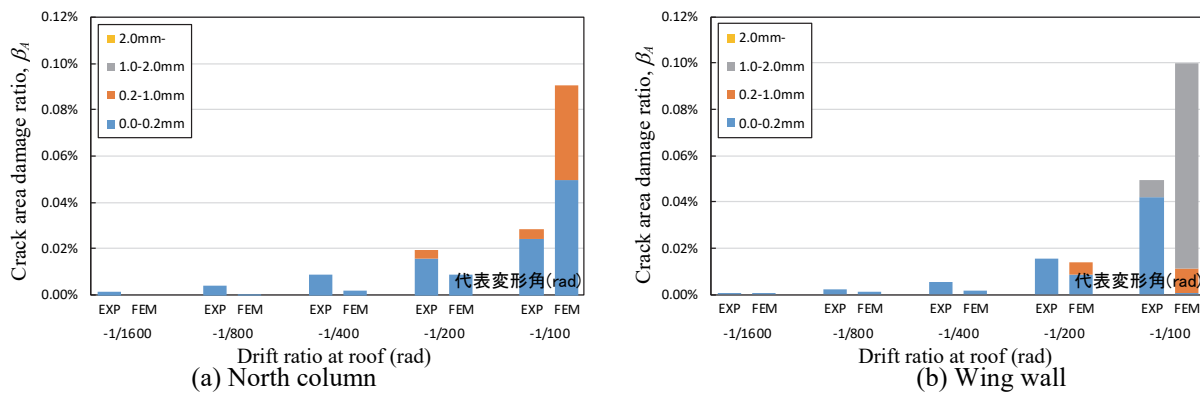


Figure 8. Comparison of experimental and computational variations of crack area damage ratio (Residual values for north column and wing wall).

Conclusions

In order to assess damage state, complete residual flexural crack profiles (crack spacing, width, and length) were simulated for the real scale five story reinforced concrete building specimen tested in 2014.

- Accumulated crack width show that crack width and spacing were well simulated for peak points of each cycles.
- Crack length can be simulated by making two assumptions; concrete does not deform, and crack is invisible if crack width is less than the limit crack width.
- Computed crack area damage ratio is not very good but tolerable up to 0.5% drift and is not good at all at 1% drift. It can be seen that the complete crack profiles such as crack damage area ratio is hard to predict even if simulated crack width profiles are not very bad.

The authors hope that simulation of complete crack profiles improves damage evaluation for serviceability and reparability limit states.

Acknowledgments

This study was carried out by a joint study of National Technology Development Project of MLIT “Development of function sustaining technologies for buildings used as Disaster Prevention Bases” (2013–2016) and Priority Research Program of BRI Development on Seismic Design Method for Building with Post Earthquake Functional Use”(2013–2015). The efforts in measuring concrete cracking by Tokyo Institute of technology, Tokyo University of Science and Tohoku University and seven

participating companies are gratefully acknowledged. A part of this study was conducted as Scientific Research A (PI: Susumu Kono) of JSPS Grant-in-Aid program. Some financial support was also granted by the World Research Hub Initiative of the Institute of Innovative Research and the Collaborative Research Project of Materials and Structures Laboratory at Tokyo Institute of Technology.

References

- Architectural Institute of Japan, Guidelines for Performance Evaluation of Earthquake Resistant Reinforced Concrete Buildings (Draft), 2004.
- CEB-FIP: Model Code for Concrete Structures, 15.2.3 Limit states of cracking, pp.156-160, 1978
- Ciampi, V. et al.: Analytical Model for Concrete Anchorages of Reinforcing Bars Under Generalized Excitations, *Report No. UCB/EERC-82/23*, Univ. of California, Berkeley, Nov., 1982
- Fukuyama, H.: Static Loading Test on A Full Scale Five Story Reinforced Concrete Building utilizing Wing Walls for Damage Reduction, *Summaries of technical papers of Annual Meeting Architectural Institute of Japan*. C-2, 2015, pp. 361-362.
- ITOCHU Techno Solutions Corporation: Science and Engineering Systems Division: *Final user's manual*, 2016
- Izumo J., Shima H., and Okamura H.: Analytical Model for Reinforced Concrete Panel Elements Subjected to In-Plane Forces, *Concrete Research and Technology*, Vol. 25 (1987), No. 9, Pp. 107-120
- JBDPA (The Japan Building Disaster Prevention Association), *Seismic Evaluation and Retrofit*, 2015
- Kabeyasawa T., Mukai T., Fukuyama H., et al.: A Full Scale Static Loading Test on Five Story Reinforced Concrete Building Utilizing Columns with Wing Walls, *Journal of Structural and Construction Engineering*, Transactions of AJJ, Vol. 81, 2016, No. 720, 313-322.
- Kabeyasawa T., Mukai T., Fukuyama H., Suwada H., and Kato H.: Full-scale static loading test on a five story reinforced concrete building, *16th World Conference on Earthquake Engineering*, Santiago Chile, January 9 – 13, 2017, Paper No. 1242
- Kitamura F.: Damage evaluation of five-story building by nonlinear finite element analysis, *Master thesis of Tokyo Instute of Technology*, 2017.
- Kono S., Kitamura F., Yuniarisyia E., Watanabe H., Mukai T., Mukai D.: Efforts to develop resilient reinforced concrete building structures in Japan, *Proceedings of the Fourth Conference on Smart Monitoring, Assessment and Rehabilitation of Civil Structures*, Sept 13-15, 2017, Zurich, Switzerland, Paper ID #KN30, 2017.
- Kono S., Kuwabara R., Kitamura F., Yuniarisyia E., Watanabe H., Mukai T., Mukai D.: Development of Resilient Reinforced Concrete Building Structural System, *Proceedings of the Sixteenth European Conference on Earthquake Engineering*, June 18-21, 2018, Thessaloniki, Greece, Paper ID #10852. 2018.
- Ministry of Land, Infrastructure, Transportation and Tourism (MLIT): *The 2015 guidelines of structural design technology of buildings*, 2015.
- Naganuma K.: Stress – strain relationship for concrete under triaxial compression, *Journal of Structural and Construction Engineering, Transactions of AJJ*, 1995, No. 474, pp. 163-170.